

ARTICLE

Tailored transgene expression to specific cell types in the central nervous system after peripheral injection with AAV9

Jonathan Dashkoff^{1,2}, Eli P Lerner², Nhi Truong², Jacob A Klickstein², Zhanyun Fan², Dakai Mu³, Casey A Maguire³, Bradley T Hyman² and Eloise Hudry²

The capacity of certain adeno-associated virus (AAV) vectors to cross the blood–brain barrier after intravenous delivery offers a unique opportunity for noninvasive brain delivery. However, without a well-tailored system, the use of a peripheral route injection may lead to undesirable transgene expression in nontarget cells or organs. To refine this approach, the present study characterizes the transduction profiles of new self-complementary AAV9 (scAAV9) expressing the green fluorescent protein (GFP) either under an astrocyte (glial fibrillary acidic (GFA) protein) or neuronal (Synapsin (Syn)) promoter, after intravenous injection of adult mice (2×10^{13} vg/kg). ScAAV9-GFA-GFP and scAAV9-Syn-GFP robustly transduce astrocytes (11%) and neurons (17%), respectively, without aberrant expression leakage. Interestingly, while the percentages of GFP-positive astrocytes with scAAV9-GFA-GFP are similar to the performances observed with scAAV9-CBA-GFP (broadly active promoter), significant higher percentages of neurons express GFP with scAAV9-Syn-GFP. GFP-positive excitatory as well as inhibitory neurons are observed, as well as motor neurons in the spinal cord. Additionally, both activated (GFAP-positive) and resting astrocytes (GFAP-negative) express the reporter gene after scAAV9-GFA-GFP injection. These data thoroughly characterize the gene expression specificity of AAVs fitted with neuronal and astrocyte-selective promoters after intravenous delivery, which will prove useful for central nervous system (CNS) gene therapy approaches in which peripheral expression of transgene is a concern.

Molecular Therapy — Methods & Clinical Development (2016) **3**, 16081; doi:10.1038/mtm.2016.81; published online 7 December 2016

INTRODUCTION

Gene therapy applied to neurodegenerative diseases is a constantly evolving field that relies on the development of efficient and safe gene delivery systems. Among many, adeno-associated virus (AAV) vectors have shown the greatest promise in the treatment of genetic or acquired diseases of the central nervous system, being generally well-tolerated and highly efficient at transducing neural cells.^{1–4} Numerous preclinical studies in rodents or nonhuman primates have achieved efficacy after AAV intraparenchymal infusion, with several clinical trials in progress.^{5–8} However, while direct cerebral injection limits the amount of vector circulating in the blood and associated potential anti-AAV immune reaction, this approach is only suitable to focally express a gene of interest, which therefore prevents its application in treating numerous diseases affecting large areas of the neural tissue. Alternatively, infusion of AAV into the intracerebroventricular, intracisternal, or intrathecal space, leads to a broader dispersion of viral particles in the cerebrospinal fluid and is especially well fitted for expressing secreted proteins throughout the brain and the spinal cord.^{9–16} While those strategies have indeed proven valuable in several neuropathological contexts, they still

involved invasive surgical procedures that may not become easily translatable to a large number of patients.

Further advances in the field have been made with the discovery of AAV serotype 9 (AAV9) ability to cross the blood–brain barrier after intravascular delivery, providing an alternative and noninvasive approach to widely express therapeutic genes across the entire central nervous system (CNS) in much larger cohorts of patients.^{17–19} The initial AAV9 findings in mice have been demonstrated to work in multiple animal models including nonhuman primates, with minimal signs of peripheral or central toxicity.^{17,20} After intravenous injection in adult animals, AAV9 primarily targets astrocytes and neurons in the CNS, with a noticeable greater astrocyte transduction from mice to non-human primates.^{19,21–23} In addition, the use of self-complementary AAV genomes, which circumvent the requirement for nascent-strand synthesis upon infection, greatly increases the efficacy of such approaches.²⁴ Preclinical studies are currently under way to assess the safety and efficiency of AAV9 for treating neurologic diseases including Alzheimer's disease (AD),²⁵ mucopolysaccharidosis IIIB,^{17,26} spinal muscular atrophy,²⁷ or amyotrophic lateral sclerosis.²⁸

The first two authors contributed equally to this work.

¹Department of Anatomy and Neurobiology, Boston University School of Medicine, Boston, Massachusetts, USA; ²MassGeneral Institute for Neurodegenerative Disease, Massachusetts General Hospital and Harvard Medical School, Charlestown, Massachusetts, USA; ³Department of Neurology, The Massachusetts General Hospital, and NeuroDiscovery Center, Harvard Medical School, Boston, Massachusetts, USA. Correspondence: E Hudry (ehudry@mgh.harvard.edu)

Received 18 August 2016; accepted 24 October 2016

Challenges associated with intravascular delivery of AAV9 include the transduction of off-target organs, the potential toxicity associated with an immune response against foreign transgene products, and the eventual side effects associated with the ectopically-expressed transgene itself.^{29,30} Although targeting multiple cell types in the CNS after intravenous delivery, AAV9 primarily transduces cells in peripheral organs including heart, liver, lung, skeletal muscle, and testes.³¹ To reduce expression in non-CNS cells, we used cell-specific promoters and developed self-complementary AAV9 vectors (scAAV9) that specifically target the expression of the green fluorescence protein (GFP) to astrocytes (using a restricted murine glial fibrillary acidic protein promoter (GFAP) or neurons (using a human synapsin promoter (Syn)). While each of those promoters has been previously used to drive AAV-dependent transgene expression selectively in neurons or astrocytes,^{32–34} no comparable study has investigated the chicken β -actin (CBA), the GFA and the Syn promoters side-by-side after scAAV9 intravenous delivery. We hypothesized that, when compared to the ubiquitously expressed hybrid CMV/CBA promoter element, both scAAV9-GFA-GFP and scAAV9-Syn-GFP would lead to targeted GFP expression of in specific sub-populations of the brain (respectively astrocytes or neurons), while greatly decreasing peripheral leakage in the liver. Additionally, the present work aimed at deciphering if those specific promoters, would indeed enrich expression of our reporter gene in a chosen neural population, outperforming a conventional vector with CBA, or simply restrict expression in astrocytes or neurons without further gain. The present study therefore explores the safety and efficacy benefit associated with a tailored AAV system to express genes specifically in the central nervous system after peripheral administration in the blood.

RESULTS

Intravenous administration of scAAV9-GFA-GFP and scAAV9-Syn-GFP result in widespread transduction of CNS, without detectable GFP signal in the liver

Because of its remarkable ability to cross the blood–brain barrier, AAV9 (as well as other AAV capsids) has been established as the vector of choice to target the central nervous system via systemic infusion. However, the safety of such systemic approach may be compromised by ectopic expression of a specific transgene in peripheral tissues. To overcome this issue and determine if we could further enhance transduction of specific cell types within the brain, we compared vectors expressing the GFP reporter gene under control of the truncated murine gfa2ABC_D promoter (GFA, astrocyte-specific), the human Synapsin promoter (Syn, neuron-specific) or the broadly active and robust hybrid CMV/CBA promoter as a control. GFA is a 681 fragment of the full-length GFAP promoter which demonstrates approximately two-fold greater activity compared to the full-length gfa2 promoter.³⁵ GFA is substantially shorter, which renders it suitable for cloning into a scAAV DNA backbone where the effective genome carrying capacity is limited to approximately 2.2 kb.³⁶ In accordance with our preliminary results (Supplementary Figure S1) as well as other studies,^{19,21} we observed a significantly higher percentage of neurons and astrocytes being transduced after injection of 2×10^{13} vg/kg of self-complementary AAV9 as opposed to its single-stranded counterpart (respective percentages of transduced neurons and astrocytes after intravenous injection of ssAAV-CBA-GFP: 0.06 ± 0.008 and $0.25 \pm 0.04\%$; respective percentages of transduced neurons and astrocytes after intravenous injection of scAAV-CBA-GFP: 2.32 ± 0.3 and $11.19 \pm 1.26\%$; nonparametric Mann-Whitney test, $P < 0.05$). We therefore designed the

next steps of our study using self-complementary AAV genomes only. Considering the limited cloning space of scAAV vectors, we also tested if coinjection or sequential injections of two scAAV-CBA encoding for a green (GFP) or a red (DsRed) reporter gene would target the same cells, thus being a suitable strategy for specific complementation approaches (1×10^{13} vg/kg for each vector, so that a total dose of 2×10^{13} vg/kg was injected altogether (Supplementary Figure S2). We observed, unfortunately, very limited cotransduction with either approach, however only one relatively low dose was attempted. This result suggests that there is not a subpopulation of neural cells that are either more closely associated with the blood–brain barrier or more susceptible to AAV to be efficiently cotransduced by two different AAV delivered peripherally at once. Because significant gender-difference of transgene expression in the brain has been reported after peripheral infusion of AAV9, we also exclusively used adult 3-month-old wild-type C57BL/6J female ($n = 4–7$ per group).³⁷ One month after intravenous injection of either vector (2×10^{13} vg/kg), immunolabeling for GFP revealed comparable widespread expression throughout the entire brain as well as spinal cord (Figure 1a). GFP-positive cells were observed in most regions of the cerebral tissue including cortex, hippocampus, striatum, and cerebellum (Figure 1b). Importantly, the presence of either the GFA or Syn promoter greatly reduced expression of the transgene in the liver (Figure 2), with no detectable GFP expressing hepatocytes as compared with the CBA promoter at the same dose. This result demonstrated that the use of CNS-selective promoters facilitates on-target transgene expression while reducing peripheral transduction.

The use of the GFA or Syn promoters restricts expression of GFP within astrocytes or neurons, respectively, after peripheral intravenous injection of scAAV9

To better characterize the cell types transduced by all three vectors, 40 μ m coronal brain sections were stained by double immunofluorescent labeling with antibodies against GFP, glutamine synthetase (GS), Neuronal Nuclei (NeuN), or ionized calcium binding adaptor molecule 1 (Iba1), respective markers for astrocytes, neurons, and microglia.^{21,38} As previously reported, both astrocytes and neurons were primarily transduced after intravenous injection of scAAV9-CBA-GFP, while no GFP-positive microglial cells could be detected. As expected, scAAV9-GFA-GFP and scAAV9-Syn-GFP restricted expression of the transgene to astrocytes or neurons, respectively, with no apparent leakiness of those promoters in other neural cell types (Figure 3).

The use of scAAV9-GFA-GFP led to GFP+/GS+ perivascular astrocytic endfeet as well as intraparenchymal astrocytes, without significant preference for cells closely located nearby blood vessels (Figure 4a). Because the GFA promoter initially derives from the murine endogenous promoter of GFAP, an intermediate filament protein which expression is regulated upon astrocyte activation, we wondered if GFA-dependent expression of GFP would be increased in GFAP-positive reactive astrocytes (*i.e.*, if the activation state of those cells could impact the expression of GFP after scAAV9-GFA-GFP injection) compared to resting (GFAP-negative astrocytes). To answer this question, scAAV9-GFA-GFP or scAAV9-CBA-GFP were injected to 7-month-old APP/PS mice, a mouse model of AD that already show substantial amyloid pathology as well as glial activation at that age (as shown by upregulation of GFAP-positive astrocytes surrounding amyloid deposits (Supplementary Figure S3)).³⁹ Inspection of immunolabeling in AD mice revealed that only a subset of GFP+ astrocytes were reactive and express GFAP, suggesting that both resting as well as activated cells could be efficiently

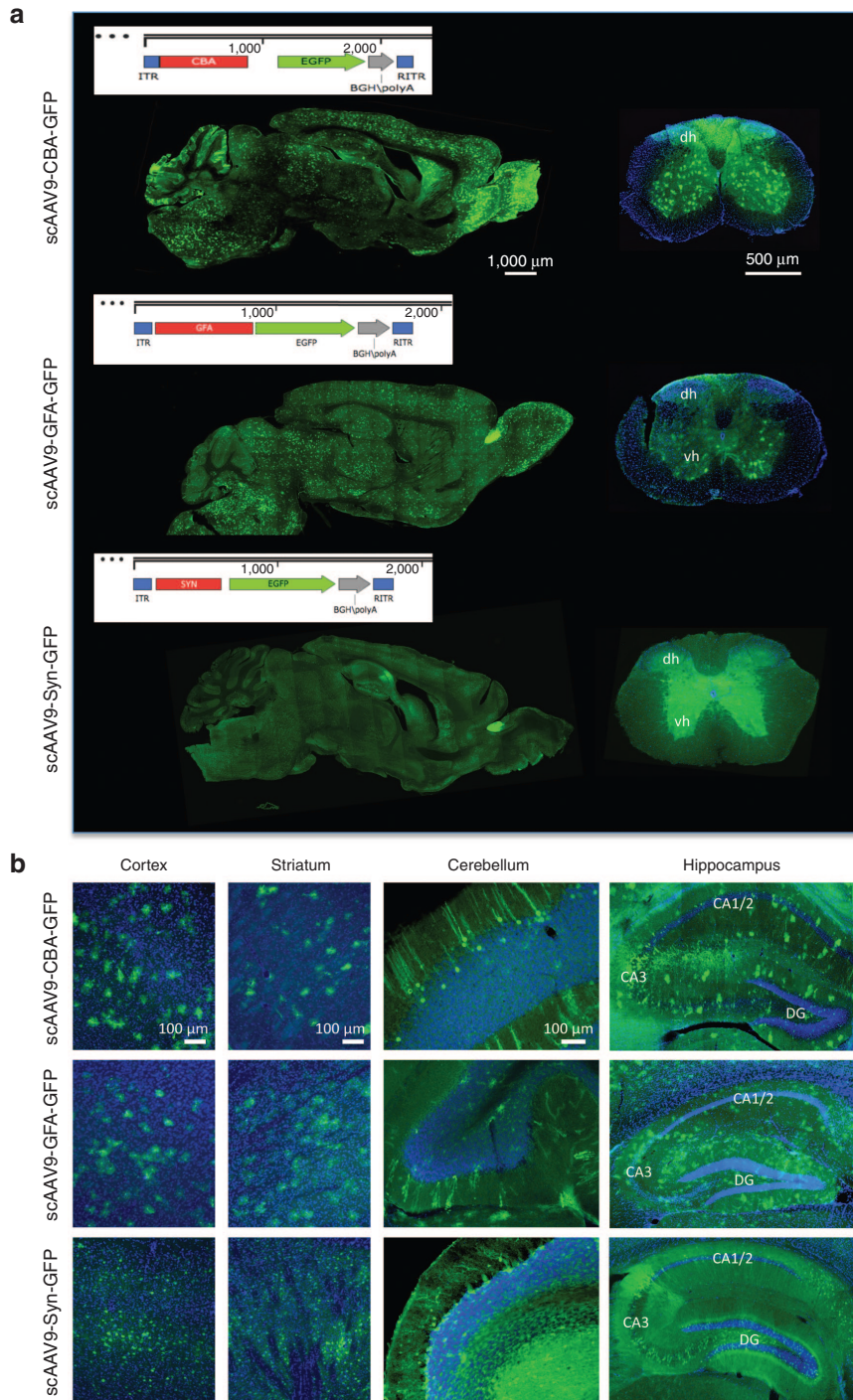


Figure 1 scAAV9-CBA-GFP, scAAV9-GFA-GFP, and scAAV9-Syn-GFP efficiently transduce the murine central nervous system after a single intravenous injection of (2×10^{13} vg/kg). **(a)** Vector maps of the scAAV expression cassettes used in the study as well as representative images of the GFP signal across an entire sagittal section of the brain after a single intravenous injection of scAAV9-CBA-GFP, scAAV9-GFA-GFP or scAAV9-Syn-GFP (left panels, scale bar = 1,000 μ m). The right panels show the overall fluorescent signal within the spinal cord after similar injections (dh and vh: dorsal and ventral horns; scale bar = 500 μ m). **(b)** A substantial number of GFP-positive cells could be detected throughout the entire cerebral tissue, as shown in the cortex, striatum, cerebellum or hippocampus (CA, Cornus Ammonis; DG, Dentate Gyrus; scale bar = 100 μ m).

targeted by scAAV9-GFA-GFP (Figure 4b). To quantitate whether scAAV9-GFA-GFP led to shift of GFP expression in reactive versus resting astrocytes, we performed a stereology-based quantification of the numbers of GFP+/GFAP+ and GFP+/GFAP- cells in the cortex. We observed a modest and nonsignificant increase in the overall number of reactive astrocytes in the cortex of mice that received

scAAV9-GFA-GFP injection compared to scAAV9-CBA-GFP. However, when the number of transduced astrocytes was normalized to the number of reactive astrocytes, there was no significant difference between vectors ($P > 0.05$, Mann-Whitney U -test, Figure 4c), leading us to conclude that there was no significant bias of expression of the AAV-GFA-GFP vector toward resting or activated astrocytes.

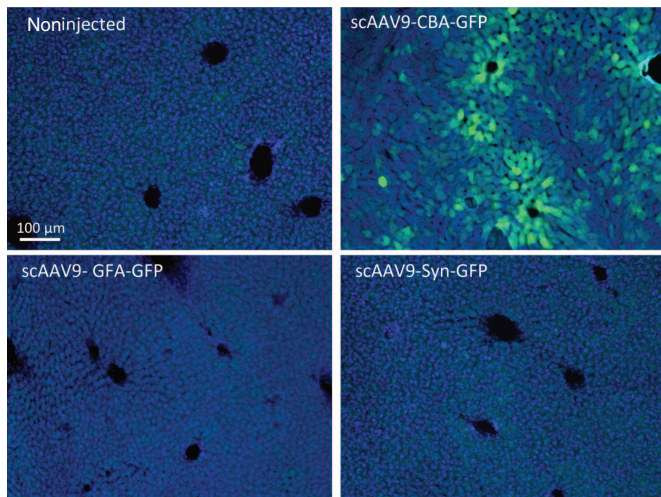


Figure 2 The presence of the GFA or a Syn promoter in the cloning cassette of scAAV9 greatly reduces expression of the transgene in hepatocytes. Representative images of liver sections after immunostaining for GFP, showing that hepatocytes are primarily transduced after intravenous injection of scAAV9-CBA-GFP. No GFP expression was detected with either the scAAV9-GFA-GFP or scAAV9-Syn-GFP (scale bar = 100 μm).

While scAAV9-GFA-GFP could lead to efficient expression of the reporter gene in phenotypically diverse astrocytes, scAAV9-Syn-GFP targeted a wide range of neuronal subtypes, including excitatory and inhibitory neurons identified by the markers CamKII or GAD67, respectively (Figure 5a,b). Few GFP-expressing Purkinje cells identified by the marker Calbindin were also observed in the cerebellum, but to a lesser extent as compared with what we previously reported using the CBA reporter²¹ (Figure 5d). In addition, GFP-expressing choline acetyltransferase-positive motor neurons were detected in the spinal cord (Figure 5e). This confirmed the broad expression profile associated with the Syn promoter, even though some important populations, such as Tyrosine Hydroxylase-positive neurons in the substantia nigra, did not seem to be efficiently targeted (Figure 5c). This transduction profile was comparable in scAAV-CBA-GFP injected mice and similar neuronal sub-populations expressed the reporter gene (data not shown).

Systemically injected scAAV9-Syn-GFP vector increases neuronal transduction compared to the CBA promoter

While our initial results indeed demonstrated the benefit of using specific cell-type promoters to target the expression of GFP in defined neural cell types, we then asked whether this tailored strategy would also correlate with an overall enrichment in the amount of astrocytes or neurons expressing our gene of interest. An unbiased stereological analysis was performed in the entire cortex to precisely quantify the percentage of astrocytes or neurons transduced after peripheral infusion of scAAV9-GFA-GFP or scAAV9-Syn-GFP as compared with our nonselective vector scAAV9-CBA-GFP (2×10^{13} vg/kg injected with each vector, Figure 6). The fraction of GFP-positive astrocytes was comparable between scAAV9-GFA-GFP and scAAV9-CBA-GFP in the cortex of wild-type 3-month-old C57BL/6J female, reaching 11.19 ± 1.26 and $11.16 \pm 1.34\%$ respectively ($P = 0.6$; nonparametric Mann-Whitney test, Figure 6b,c, left panels). By contrast, the percentage of GFP-positive neuronal cells detected with scAAV9-Syn-GFP ($16.75 \pm 2.28\%$) was dramatically higher than with scAAV9-CBA-GFP ($2.32 \pm 0.3\%$) ($P = 0.0061$; nonparametric

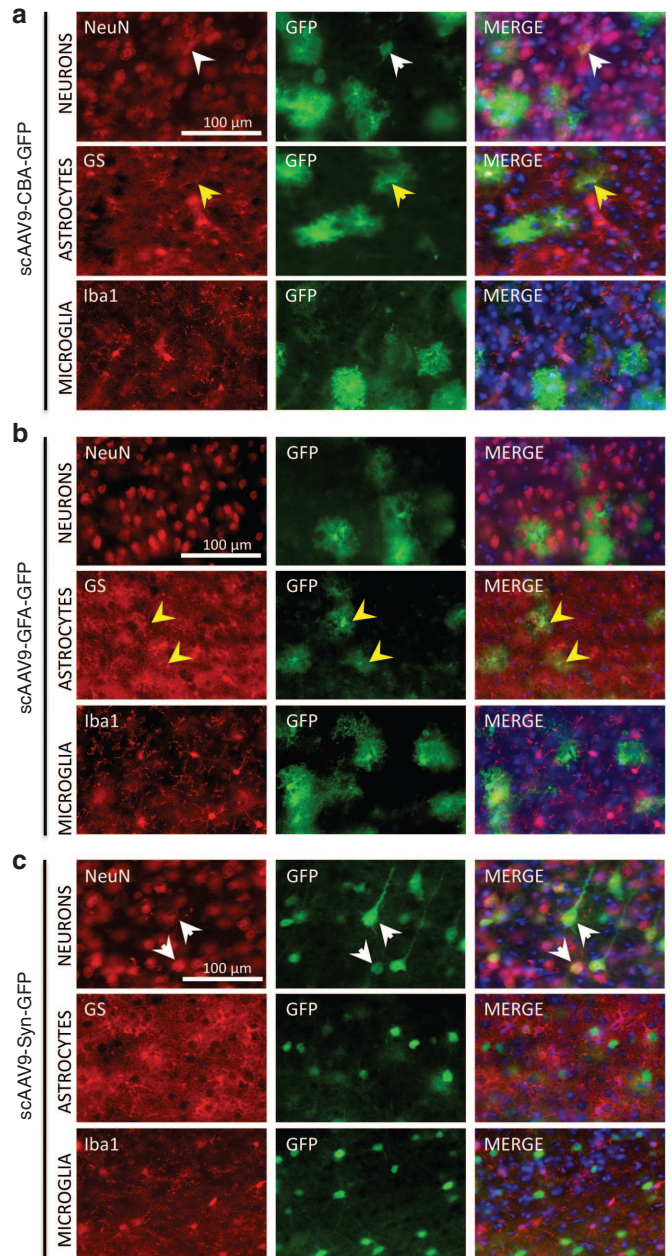


Figure 3 The presence of the GFA or Syn promoter restricts expression of GFP in astrocytes or neurons, respectively. Representative images of coimmunostaining for GFP-expressing cells with cellular markers of neurons (NeuN), astrocytes (GS), or microglia (Iba-1) after peripheral injection of scAAV9-CBA-GFP (a), scAAV9-GFA-GFP (b), or scAAV9-Syn-GFP (c). Neurons (white arrowheads) and astrocytes (yellow arrowheads) were concomitantly transduced after intravenous infusion of adult wild-type mice with the ubiquitous scAAV9-CBA-GFP, while no GFP-positive microglial cells could be observed. As expected, the presence of the GFA or the Syn promoter specifically restricted GFP expression to astrocytes or neurons, respectively. All pictures were taken in the cortex; scale bar = 100 μm.

Mann-Whitney test, Figure 6b,c, right panels). Because the insertion of a Syn promoter did not impact the overall transduction profile of neuronal subtypes, we hypothesize that activity levels may differ between the Syn and CBA promoters in neurons in general, although it is possible that the Syn promoter in particular subtypes is more active than CBA compared to other subtypes.

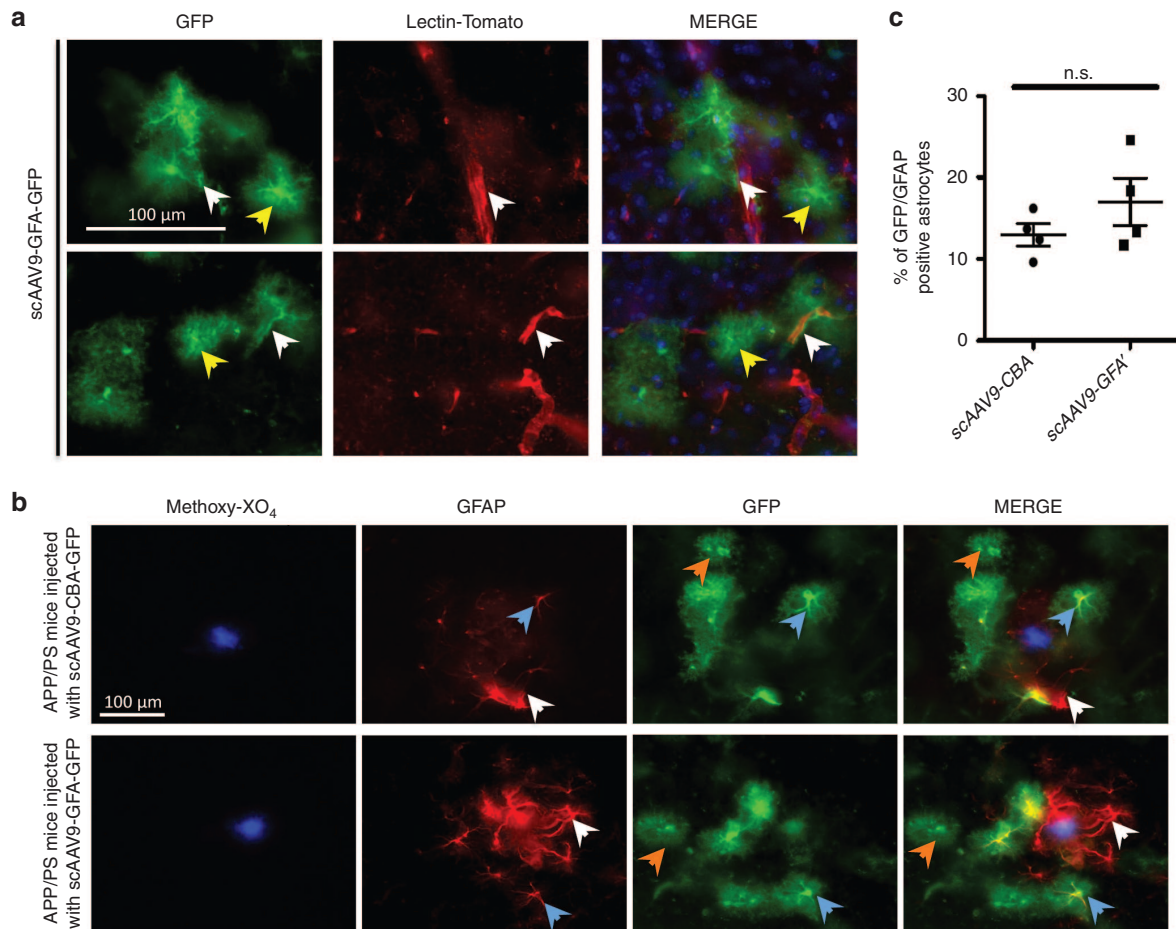


Figure 4 scAAV9-GFA-GFP mediates GFP expression in resting or activated astrocytes. **(a)** Representative images of GFP-transduced astrocytes together with capillaries (stained with lectin-tomato), showing that astrocytic endfeet (white arrows) as well as parenchymal astrocytes (yellow arrows) were evenly transduced by scAAV9-GFA-GFP. **(b)** When scAAV9-GFA-GFP was injected in the lateral tail vein of 7 month-old APP/PS mice, we observed that both resting (GFAP-negative, orange arrows) and activated (GFAP-positive, blue arrows) astrocytes expressed GFP. Additionally, numerous GFAP-positive astrocytes surrounding each amyloid deposit (labeled via intravenous injection of the PiB derivative Methoxy-XO₄) did not express the reporter gene (white arrows). **(c)** Stereological evaluation of the percentage of reactive astrocytes expressing the reporter gene after iv injection of scAAV9-CBA-GFP or scAAV9-GFA-GFP demonstrated that GFA-dependent expression of GFP was independent upon the activation state of those cells (cortex, scale bar = 100 μm).

DISCUSSION

The present study investigated the benefit associated with the use of specific neural cell promoters, namely GFA or Syn, in order to target expression of a reporter gene in astrocytes or neurons after a single intravenous infusion of self-complementary AAV9 in adult immunocompetent wild-type mice. In agreement with previous data,²³ we found self-complementary vectors to vastly outperform single stranded vectors in the expression of GFP in the context of AAV9 capsid. The underlying mechanisms of this discrepancy between single- and double-stranded AAV genomes remain partially unresolved. However, previous work has suggested that this effect may be related with the rate-limiting conversion of ssDNA to double-stranded genomic DNA, a slow process that relies on host-cell DNA synthesis and delays or impairs transduction.^{40,41} Conversely, the packaging capacity of scAAV vectors only reaches 2.2 kb, which will obviously prevent the cloning of numerous therapeutic genes much larger than GFP.³⁶ This constitutes a major drawback when applying the present strategy to various diseases, and our results also demonstrated that either coinjection or sequential infusion of two scAAV9 targeted a very low number of the same cells in the CNS. However, we only injected a relatively low dose (2×10^{13} vg/kg)

and increasing the dose by an order of magnitude would likely increase cotransduction percentages. Also, newly developed AAV variants such as AAV-PHP.B will potentially overcome this issue when used at high doses, as they have been associated with remarkable transduction efficacy even after peripheral administration of single-stranded AAV vector (reaching up to 80% of transduction in astrocytes²²). Alternatively, direct intracerebral injection of two AAV has previously been shown to successfully achieve cotransduction of the same cells.⁴² Despite the low percentage cotransduced (~4%) at the dose tested, our data reveal some interesting findings. First, since the coinjection protocol was a 1:1 ratio of AAVs encoding GFP or DsRed, if high vg/cell were required for functional transduction, we would see more cotransduced cells. As ~96% of neural cells were either red or green at this dose, our results indicate that functional transduction with systemically administered AAV can be achieved at very low vg/cell, perhaps as low as 1 vg/cell. The other interesting finding with low cotransduction is that, at the dose and brain regions examined, no particular “transduction susceptibility” of particular neural cells over others was observed.

Even though intravenous infusion of AAV has the potential to achieve transduction of large areas and may be an approach of

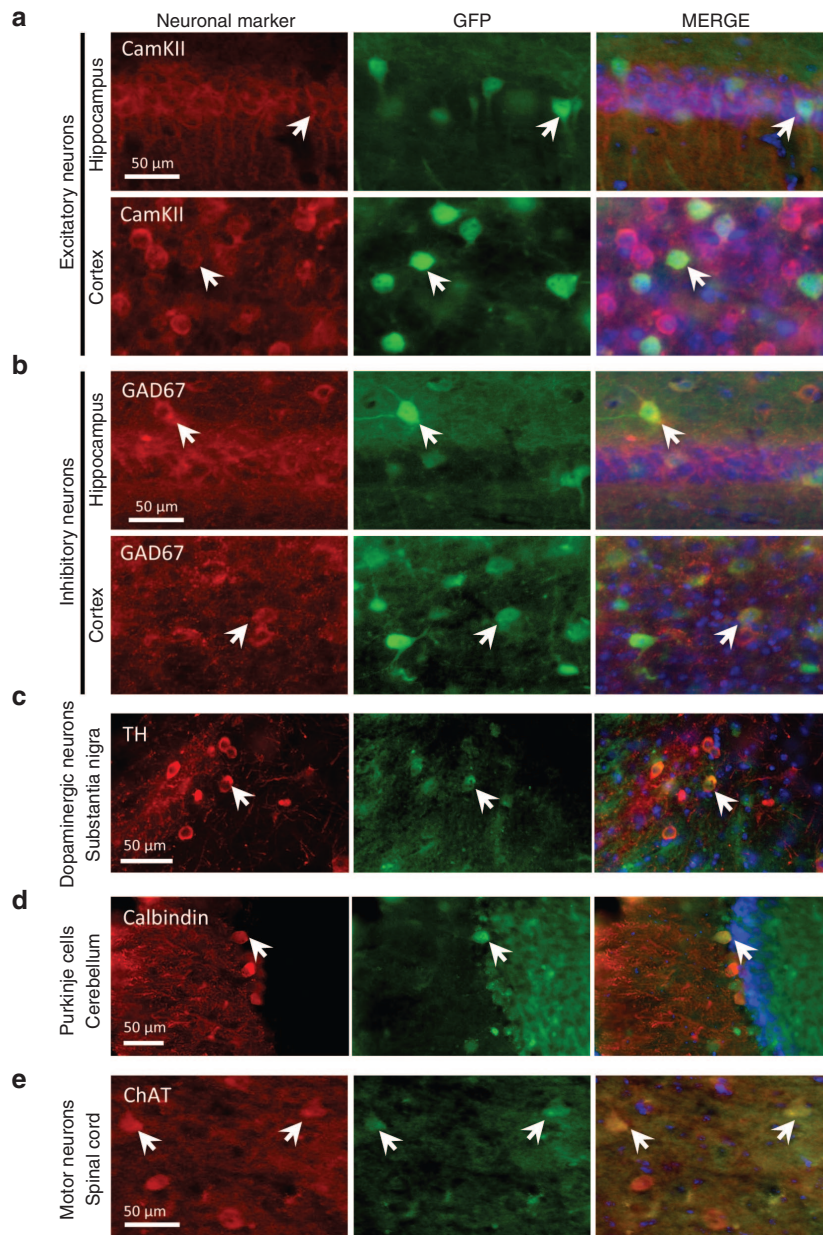


Figure 5 scAAV9-Syn-GFP allows expression of a specific transgene in various neuronal subtypes. Peripheral infusion of scAAV9-Syn-GFP led to efficient transduction of both excitatory (**a**) as well as inhibitory (**b**) neurons (respectively identified by the CamKII and GAD67 markers). TH-positive neurons in the substantia nigra rarely expressed GFP (**c**). Few transduced Purkinje cells could also be observed in the cerebellum (**d**), their density being much lower as compared with what has been previously reported using a CBA promoter.²¹ Importantly, ChAT-positive motor neurons expressing GFP were also observed in the spinal cord (**e**). CamKII, Ca²⁺/calmodulin-dependent protein kinase II; ChAT, choline acetyltransferase; GAD67, glutamic acid decarboxylase; TH, tyrosine hydroxylase; scale bar = 50 μm.

choice for specific diseases broadly affecting the central nervous system, one downside is the resulting expression of multiple non-CNS tissues.³¹ By driving expression of the GFP reporter gene under a fragment of the murine truncated GFA promoter or a human synapsin promoter, we successfully restricted expression to astrocytes or neurons in the brain after AAV9 intravenous injection. Of importance, no GFP-positive hepatocytes could be detected in the liver tissue by immunohistological analysis, thus emphasizing on our ability to target expression of the transgene into the brain and spinal cord only. While we cannot rule out that higher doses of AAV may lead to some leakiness of expression in the periphery, our results show greatly reduced expression relative to broadly active

promoters (*i.e.*, CBA). This could allow safer use of AAV vector for clinical applications, as previous gene therapy trials have reported the possible development of host immune responses against the transgene product, especially when the protein is initially absent in patients.^{43,44}

When the percentage GFP-expressing cells in the cortex was evaluated by unbiased stereology-based quantification, we demonstrated that the use of restricted promoters to narrow gene expression in astrocytes or neurons did not decrease the overall transduction efficiency of those targeted cell populations compared to the more ubiquitous CBA promoter. We observed that scAAV9-GFA and scAAV9-CBA achieved similar transduction levels in astrocytes after

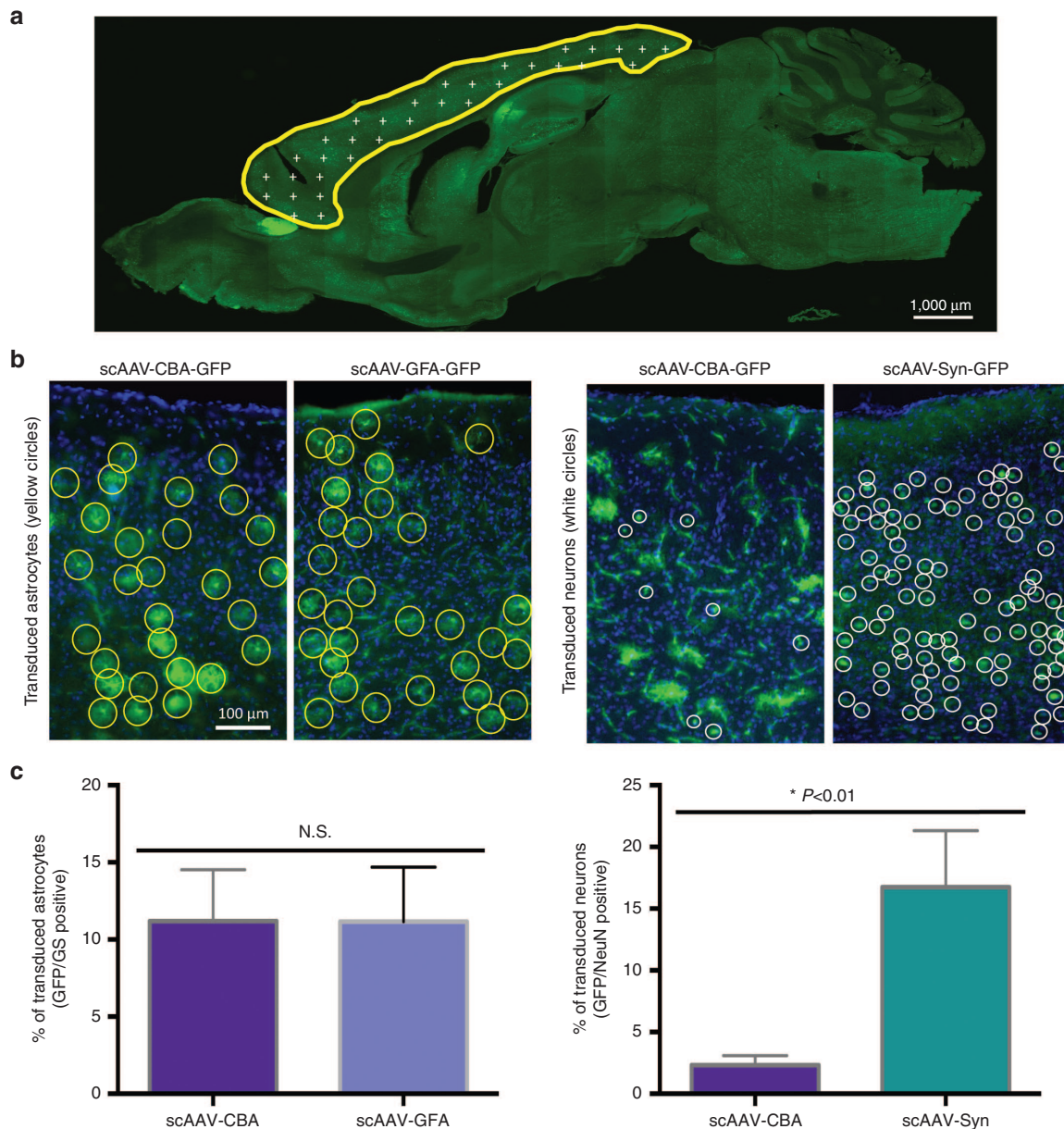


Figure 6 Addition of a specific neuronal promoter significantly enhances GFP expression in neurons as compared with the CBA promoter. (a) An unbiased stereological analysis of the percentages of astrocytes and neurons, respectively identified by the markers Glutamine Synthetase and NeuN, was performed in the cortex of scAAV-GFA-GFP or scAAV9-Syn-GFP. (b) Representative images showing the density of GFP-positive astrocytes (yellow circles) or neurons (white circles) in the cortex after peripheral infusion of scAAV9-CBA-GFP, scAAV9-GFA-GFP or scAAV9-Syn-GFP. (c) While the use of either CBA or GFA promoter leads to similar levels of transduced astrocytes, the presence of a Syn promoter increases the level of GFP-positive neurons by a factor of 4 ($n = 6$ for scAAV9-CBA-GFP; $n = 6$ for scAAV9-GFA-GFP, and $n = 4$ for scAAV9-Syn-GFP, nonparametric Mann-Whitney test).

intravenous infusion of vector at a dose of 2×10^{13} vg/kg, and targeted astrocytes were evenly distributed throughout the neural tissue. Interestingly, there was no preferential transduction of cells closely connected with blood vessels as opposed to parenchymal astrocytes. In addition, both activated and resting astrocytes expressed GFP when scAAV9 vectors were injected in APP/PS mice models of Alzheimer’s disease that showed substantial astrocytic activation, a result of particular relevance when applied to neurological diseases that are often associated with increased reactive gliosis.^{45,46} By contrast, the comparison of neuronal transduction after intravascular injection of scAAV9-CBA-GFP or scAAV9-Syn-GFP revealed a significant increase in GFP-positive neurons when using a specific human Synapsin promoter as opposed with CBA. CBA is

generally a robust promoter and is considered to be “ubiquitously” expressed. However, our data suggest that in some cases, quintessential strong, ubiquitous promoters such as CBA do not always have the highest activity in the target cell. This is supported by data showing different transduction patterns of two different strong promoters, CBA and CMV, in the mouse retina.⁴⁷ In the future, it may be possible to enhance neuronal targeting even further by combining the transcriptional targeting described here with neuron-targeted AAV capsids.⁴⁸

The present study therefore emphasizes on the benefit of designing AAV genomic backbones with narrowed expression abilities for CNS gene therapy approaches in which peripheral expression of transgene is a concern. While the present study used an AAV9

serotype, one can assume that our findings (difference between ssAAV and scAAV backbone, restricted expression of a specific transgene using specific promoters, are generalizable to other AAV serotypes that have been shown to cross the blood–brain barrier after intravenous delivery, such as rAAVrh.8, rAAVrh.10, or AAV-PHP.B.^{22,49}

MATERIALS AND METHODS

Viral vector construction and production

Four AAV backbones driving the expression of GFP were used in these experiments, as well as one AAV backbone leading to the expression of DsRed (for the experiments of co- and sequential injection between scAAV9-CBA-GFP and scAAV9-CBA-DsRed). ssAAV9-CBA-GFP and scAAV9-CBA-GFP were kindly provided by Bakhos Tannous (MGH vector core), driving expression of GFP under the hybrid CMV/CBA promoter. scAAV9-GFA-GFP and scAAV9-Syn-GFP were constructed by cloning the gfaABC(1)D promoter (generously provided by Dr. Bryan Roth, The University of North Carolina, (Addgene #50473)³⁵), or the human Syn promoter (provided by Penn vector core, University of Pennsylvania, the sequence is available from Addgene, Ref. #50465) in place of CBA (Digestion MluI/NcoI). AAV serotype 9 vectors were produced as described previously.³⁷ Briefly, 293T were transfected with AAV plasmids (AAV9 rep/cap and scAAV-ITR containing transgene expression plasmid) and helper plasmid (pAdΔF6) by the calcium phosphate method. Seventy-two hours post-transfection, cells were harvested and vector purified using a iodixanol density-gradient and ultracentrifugation protocol. Iodixanol was removed and vector concentrated in phosphate-buffered saline (PBS) by diafiltration using Amicon Ultra 100 kDa Molecular weight cut-off centrifugal devices (Millipore, Billerica, MA). The AAV viral titers expressed as viral genomes/ml were determined by quantitative real-time PCR and the vectors were stored at -80°C until use.

Animals and intravenous injections of AAVs

Three-month-old wild-type female C57BL/6J mice were purchased from Jackson Laboratory (Bar Harbor, ME) and used for the major part of the study. In order to determine the capacity of scAAV9 at transducing activated GFAP-positive astrocytes, 7-month-old APP/PS transgenic mice (strain B6C3-Tg (APP^{swe}, PSEN1^{dE9}) 85Dbo/J),⁵⁰ from Jackson Laboratory) were chosen. A human mutant amyloid precursor protein gene containing the Swedish double mutation K594N/M595L was inserted in the genome of these two mouse lines, under the control of the prion protein promoter. In addition, the APP/PS1 mouse model overexpresses a variant of the Presenilin 1 gene deleted for the exon 9 (driven by the same promoter). The concomitant overexpression of APP^{swe} and PSEN1 in APP/PS1 mice leads to a more severe phenotype, with substantial amyloid deposition visible as soon as 6 months of age. Because we previously reported a significant difference of transduction after intravenous injection of scAAV9 in males versus female, the entire study was conducted using females only.³⁷ Mice were injected intravenously through the lateral tail vein with (2×10^{13} vg/kg in a final volume of 250 μl of sterile PBS) and the virus was allowed to express for 4 weeks before euthanasia. APP/PS1 mice were sacrificed after intravenous injection of the PiB derivative Methoxy-XO₄ (5 mg/kg) in order to visualize amyloid plaques. All studies were performed with the approval of the Massachusetts General Hospital Animal Care and Use Committee and in compliance with the National Institute of Health guidelines for the use of experimental animals.

Tissue collection and processing

Mice were euthanized by CO₂ asphyxiation and tissue collected for immunohistochemical analyses. One cerebral hemisphere was and peripheral organs were fixed by immersion in 4% paraformaldehyde and 15% glycerol in PBS for 48 hours before cryoprotection with 30% glycerol in PBS. These samples were subsequently sectioned on a freezing microtome into 40- μm -thick sections. For immunohistochemistry and stereological analyses, brains were sectioned in the sagittal plane into 10 series.

Immunohistochemistry

Floating sections were immunolabeled with antibodies directed against GFP, GFAP, GS, NeuN, Iba-1, CaMKII- β , GAD67, or choline acetyltransferase. Primary and secondary antibodies used in experiments are listed in Supplementary Table S1. First, sections were rinsed briefly in tris-buffered saline (TBS) to remove the excess of glycerol and then were permeabilized

in 0.5% TritonX in TBS for 20 minutes at room temperature. Sections were washed three times for 10 minutes each time, blocked with 5% normal goat serum and 0.5% TritonX in TBS for 1 hour at room temperature, and then incubated with primary antibody overnight at 4°C in 2.5% normal goat serum and 0.1% Triton in TBS. Sections were washed with TBS and incubated with appropriate secondary antibody in 2.5% normal goat serum and 0.1% TritonX in TBS. After another round of washing, sections were mounted onto slides and coverslipped with Vectashield mounting medium containing the nuclear dye 4',6'-diamidino-2-phenylindole (DAPI) (Vector Labs, Burlingame, CA) or with DAPI Fluoromount-G (SouthernBiotech, Birmingham, AL). Images were collected on a Zeiss Axio Imager 2 epifluorescent microscope equipped with Coolsnap digital camera (Photometrics, Tucson, AZ) and AxioVision software (Zeiss).

Stereology-based quantitative analyses

Stereology-based studies were performed on immunolabeled sections using an Olympus BX52 epifluorescent microscope equipped with motorized stage, DP70 digital CCD camera, and CAST stereology software (Olympus, Tokyo, Japan). The cortex was outlined under low power objective (4x) and astrocytes and neurons counts were made using a 20×0.75 numerical aperture objective, with a meander sampling of the selected cortical area. We generally used different probes in order to quantify the overall density of neurons and astrocytes (probe = 5%) and the amount of GFP-positive neurons or astrocytes (probe = 10%). Estimates of the numbers of transduced neurons and astrocytes (by immunolabeling and morphology) were calculated using the fractionator method.

Statistics

Pairwise comparisons were performed using the non-parametric Mann-Whitney *U*-test. For comparing more than two groups, the nonparametric Kruskal-Wallis test was performed followed by *post-hoc* tests, if necessary. We used nonparametric tests, as the D'Agostino and Pearson normality test was not conclusive due to the small sizes of our experimental groups. The significance level was set at $\alpha = 0.05$. All the results are presented as the mean with standard deviation. All statistical analyses were performed using GraphPad Prism for Mac software version 5.0 (GraphPad Software, La Jolla, CA).

ACKNOWLEDGMENTS

This work was supported by NIA K99 AG047336, the Alzheimer's Drug Discovery Foundation (E.H.), NIH/NINDS R21 NS081374-01 (C.M.), an American Brain Tumor Association Discovery grant (C.M.), and JPB Foundation (B.T.H.).

REFERENCES

- Craig, AJ and Housley, GD (2016). Evaluation of gene therapy as an intervention strategy to treat brain injury from stroke. *Front Mol Neurosci* **9**: 34.
- Gessler, DJ and Gao, G (2016). Gene therapy for the treatment of neurological disorders: metabolic disorders. *Methods Mol Biol* **1382**: 429–465.
- Bourdenx, M, Duthel, N, Bezard, E and Dehay, B (2014). Systemic gene delivery to the central nervous system using adeno-associated virus. *Front Mol Neurosci* **7**: 50.
- Gelfand, Y and Kaplitt, MG (2013). Gene therapy for psychiatric disorders. *World Neurosurg* **80**: S32.e11–S32.e18.
- Bennett, J, Ashtari, M, Wellman, J, Marshall, KA, Cycowski, LL, Chung, DC *et al.* (2012). AAV2 gene therapy readministration in three adults with congenital blindness. *Sci Transl Med* **4**: 120ra15.
- Maguire, AM, High, KA, Auricchio, A, Wright, JF, Pierce, EA, Testa, F *et al.* (2009). Age-dependent effects of RPE65 gene therapy for Leber's congenital amaurosis: a phase 1 dose-escalation trial. *Lancet* **374**: 1597–1605.
- Worgall, S, Sondhi, D, Hackett, NR, Kosofsky, B, Kekatpure, MV, Neyzi, N *et al.* (2008). Treatment of late infantile neuronal ceroid lipofuscinosis by CNS administration of a serotype 2 adeno-associated virus expressing CLN2 cDNA. *Hum Gene Ther* **19**: 463–474.
- Janson, C, McPhee, S, Bilaniuk, L, Haselgrove, J, Testaiuti, M, Freese, A *et al.* (2002). Clinical protocol. Gene therapy of Canavan disease: AAV-2 vector for neurosurgical delivery of aspartoacylase gene (ASPA) to the human brain. *Hum Gene Ther* **13**: 1391–1412.
- Guo, Y, Wang, D, Qiao, T, Yang, C, Su, Q, Gao, G *et al.* (2016). A single injection of recombinant adeno-associated virus into the lumbar cistern delivers transgene expression throughout the whole spinal cord. *Mol Neurobiol* **53**: 3235–3248.
- Hironaka, K, Yamazaki, Y, Hirai, Y, Yamamoto, M, Miyake, N, Miyake, K *et al.* (2015). Enzyme replacement in the CSF to treat metachromatic leukodystrophy in mouse model using

- single intracerebroventricular injection of self-complementary AAV1 vector. *Sci Rep* **5**: 13104.
11. Hordeaux, J, Dubreil, L, Deniaud, J, Iacobelli, F, Moreau, S, Ledevin, M et al. (2015). Efficient central nervous system AAVrh10-mediated intrathecal gene transfer in adult and neonate rats. *Gene Ther* **22**: 316–324.
 12. Hinderer, C, Bell, P, Gurda, BL, Wang, Q, Louboutin, JP, Zhu, Y et al. (2014). Intrathecal gene therapy corrects CNS pathology in a feline model of mucopolysaccharidosis I. *Mol Ther* **22**: 2018–2027.
 13. Haurigot, V, Marcó, S, Ribera, A, Garcia, M, Ruza, A, Villacampa, P et al. (2013). Whole body correction of mucopolysaccharidosis IIIA by intracerebrospinal fluid gene therapy. *J Clin Invest* **123**(8): 3254–71.
 14. Hudry, E, Dashkoff, J, Roe, AD, Takeda, S, Koffie, RM, Hashimoto, T et al. (2013). Gene transfer of human Apoe isoforms results in differential modulation of amyloid deposition and neurotoxicity in mouse brain. *Sci Transl Med* **5**: 212ra161.
 15. Levites, Y, Jansen, K, Smithson, LA, Dakin, R, Holloway, VM, Das, P et al. (2006). Intracranial adeno-associated virus-mediated delivery of anti-pan amyloid beta, amyloid beta40, and amyloid beta42 single-chain variable fragments attenuates plaque pathology in amyloid precursor protein mice. *J Neurosci* **26**: 11923–11928.
 16. Beutler, AS, Banck, MS, Walsh, CE, and Milligan, ED (2005). Intrathecal gene transfer by adeno-associated virus for pain. *Curr Opin Mol Ther* **7**: 431–439.
 17. Murrey, DA, Naughton, BJ, Duncan, FJ, Meadows, AS, Ware, TA, Campbell, KJ et al. (2014). Feasibility and safety of systemic rAAV9-hNAGLU delivery for treating mucopolysaccharidosis IIIB: toxicology, biodistribution, and immunological assessments in primates. *Hum Gene Ther Clin Dev* **25**: 72–84.
 18. Mattar, CN, Waddington, SN, Biswas, A, Johana, N, Ng, XW, Fisk, AS et al. (2013). Systemic delivery of scAAV9 in fetal macaques facilitates neuronal transduction of the central and peripheral nervous systems. *Gene Ther* **20**: 69–83.
 19. Foust, KD, Nurre, E, Montgomery, CL, Hernandez, A, Chan, CM and Kaspar, BK (2009). Intravascular AAV9 preferentially targets neonatal neurons and adult astrocytes. *Nat Biotechnol* **27**: 59–65.
 20. Pleger, ST, Shan, C, Ksienzyk, J, Bekeredjian, R, Boekstegers, P, Hinkel, R et al. (2011). Cardiac AAV9-S100A1 gene therapy rescues post-ischemic heart failure in a preclinical large animal model. *Sci Transl Med* **3**: 92ra64.
 21. Hudry, E, Martin, C, Gandhi, S, György, B, Scheffer, DI, Mu, D et al. (2016). Exosome-associated AAV vector as a robust and convenient neuroscience tool. *Gene Ther* **23**: 380–392.
 22. Deverman, BE, Pravdo, PL, Simpson, BP, Kumar, SR, Chan, KY, Banerjee, A et al. (2016). Cre-dependent selection yields AAV variants for widespread gene transfer to the adult brain. *Nat Biotechnol* **34**: 204–209.
 23. Gray, SJ, Matagne, V, Bachaboina, L, Yadav, S, Ojeda, SR and Samulski, RJ (2011). Preclinical differences of intravascular AAV9 delivery to neurons and glia: a comparative study of adult mice and nonhuman primates. *Mol Ther* **19**: 1058–1069.
 24. McCarty, DM (2008). Self-complementary AAV vectors; advances and applications. *Mol Ther* **16**: 1648–1656.
 25. Iwata, N, Sekiguchi, M, Hattori, Y, Takahashi, A, Asai, M, Ji, B et al. (2013). Global brain delivery of neprilysin gene by intravascular administration of AAV vector in mice. *Sci Rep* **3**: 1472.
 26. Fu, H, Dirosario, J, Killedar, S, Zaraspe, K and McCarty, DM (2011). Correction of neurological disease of mucopolysaccharidosis IIIB in adult mice by rAAV9 trans-blood-brain barrier gene delivery. *Mol Ther* **19**: 1025–1033.
 27. Benkhalifa-Ziyyat, S, Besse, A, Roda, M, Duque, S, Astord, S, Carcenac, R et al. (2013). Intramuscular scAAV9-SMN injection mediates widespread gene delivery to the spinal cord and decreases disease severity in SMA mice. *Mol Ther* **21**: 282–290.
 28. Yamashita, T, Chai, HL, Teramoto, S, Tsuji, S, Shimazaki, K, Muramatsu, S et al. (2013). Rescue of amyotrophic lateral sclerosis phenotype in a mouse model by intravenous AAV9-ADAR2 delivery to motor neurons. *EMBO Mol Med* **5**: 1710–1719.
 29. Sarukhan, A, Camugli, S, Gjata, B, von Boehmer, H, Danos, O and Jooss, K (2001). Successful interference with cellular immune responses to immunogenic proteins encoded by recombinant viral vectors. *J Virol* **75**: 269–277.
 30. Brockstedt, DG, Podsakoff, GM, Fong, L, Kurtzman, G, Mueller-Ruchholtz, W and Engleman, EG (1999). Induction of immunity to antigens expressed by recombinant adeno-associated virus depends on the route of administration. *Clin Immunol* **92**: 67–75.
 31. Zicarelli, C, Soltys, S, Rengo, G and Rabinowitz, JE (2008). Analysis of AAV serotypes 1–9 mediated gene expression and tropism in mice after systemic injection. *Mol Ther* **16**: 1073–1080.
 32. Huda, F, Konno, A, Matsuzaki, Y, Goenawan, H, Miyake, K, Shimada, T et al. (2014). Distinct transduction profiles in the CNS via three injection routes of AAV9 and the application to generation of a neurodegenerative mouse model. *Mol Ther Methods Clin Dev* **1**: 14032.
 33. Lawlor, PA, Bland, RJ, Mouravlev, A, Young, D and During, MJ (2009). Efficient gene delivery and selective transduction of glial cells in the mammalian brain by AAV serotypes isolated from nonhuman primates. *Mol Ther* **17**: 1692–1702.
 34. Kügler, S, Kilic, E and Bähr, M (2003). Human synapsin 1 gene promoter confers highly neuron-specific long-term transgene expression from an adenoviral vector in the adult rat brain depending on the transduced area. *Gene Ther* **10**: 337–347.
 35. Lee, Y, Messing, A, Su, M and Brenner, M (2008). GFAP promoter elements required for region-specific and astrocyte-specific expression. *Glia* **56**: 481–493.
 36. Wu, J, Zhao, W, Zhong, L, Han, Z, Li, B, Ma, W et al. (2007). Self-complementary recombinant adeno-associated viral vectors: packaging capacity and the role of rep proteins in vector purity. *Hum Gene Ther* **18**: 171–182.
 37. Maguire, CA, Crommentuijn, MH, Mu, D, Hudry, E, Serrano-Pozo, A, Hyman, BT et al. (2013). Mouse gender influences brain transduction by intravascularly administered AAV9. *Mol Ther* **21**: 1470–1471.
 38. Anlauf, E and Derouiche, A (2013). Glutamine synthetase as an astrocytic marker: its cell type and vesicle localization. *Front Endocrinol (Lausanne)* **4**: 144.
 39. Kraft, AW, Hu, X, Yoon, H, Yan, P, Xiao, Q, Wang, Y et al. (2013). Attenuating astrocyte activation accelerates plaque pathogenesis in APP/PS1 mice. *FASEB J* **27**: 187–198.
 40. Wang, Z, Ma, HI, Li, J, Sun, L, Zhang, J and Xiao, X (2003). Rapid and highly efficient transduction by double-stranded adeno-associated virus vectors *in vitro* and *in vivo*. *Gene Ther* **10**: 2105–2111.
 41. McCarty, DM, Monahan, PE and Samulski, RJ (2001). Self-complementary recombinant adeno-associated virus (scAAV) vectors promote efficient transduction independently of DNA synthesis. *Gene Ther* **8**: 1248–1254.
 42. Bosch, MK, Nerbonne, JM and Ornitz, DM (2014). Dual transgene expression in murine cerebellar Purkinje neurons by viral transduction *in vivo*. *PLoS One* **9**: e104062.
 43. Mingozi, F and High, KA (2013). Immune responses to AAV vectors: overcoming barriers to successful gene therapy. *Blood* **122**: 23–36.
 44. Zaiss, AK and Muruve, DA (2005). Immune responses to adeno-associated virus vectors. *Curr Gene Ther* **5**: 323–331.
 45. Verkhatsky, A, Parpura, V, Pekna, M, Pekny, M and Sofroniew, M (2014). Glia in the pathogenesis of neurodegenerative diseases. *Biochem Soc Trans* **42**: 1291–1301.
 46. Maragakis, NJ and Rothstein, JD (2006). Mechanisms of disease: astrocytes in neurodegenerative disease. *Nat Clin Pract Neurol* **2**: 679–689.
 47. Xiong, W and Cepko, C (2016). Distinct expression patterns of AAV8 vectors with broadly active promoters from subretinal injections of neonatal mouse eyes at two different ages. *Adv Exp Med Biol* **854**: 501–507.
 48. Choudhury, SR, Harris, AF, Cabral, DJ, Keeler, AM, Sapp, E, Ferreira, JS et al. (2016). Widespread central nervous system gene transfer and silencing after systemic delivery of novel AAV-AS vector. *Mol Ther* **24**: 726–735.
 49. Yang, B, Li, S, Wang, H, Guo, Y, Gessler, DJ, Cao, C et al. (2014). Global CNS transduction of adult mice by intravenously delivered rAAVrh.8 and rAAVrh.10 and nonhuman primates by rAAVrh.10. *Mol Ther* **22**: 1299–1309.
 50. Borchelt, DR, Ratovitski, T, van Lare, J, Lee, MK, Gonzales, V, Jenkins, NA et al. (1997). Accelerated amyloid deposition in the brains of transgenic mice coexpressing mutant presenilin 1 and amyloid precursor proteins. *Neuron* **19**: 939–945.



This work is licensed under a Creative Commons Attribution-NonCommercial-NoDerivs 4.0 International License. The images or other third party material in this article are included in the article's Creative Commons license, unless indicated otherwise in the credit line; if the material is not included under the Creative Commons license, users will need to obtain permission from the license holder to reproduce the material. To view a copy of this license, visit <http://creativecommons.org/licenses/by-nc-nd/4.0/>

© The Author(s) (2016)

Supplementary Information accompanies this paper on the *Molecular Therapy—Methods & Clinical Development* website (<http://www.nature.com/mtm>)